RSC Advances

ROYAL SOCIETY OF CHEMISTRY

www.rsc.org/advances

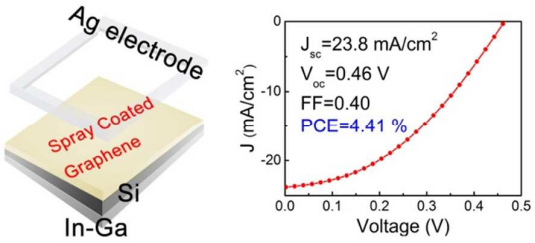

A facile method – graphene on silicon (G/Si) solar cells prepared by spray coating is developed. The power conversion efficiency (PCE) of spray-coated G/Si solar cells can reach 4.41%, comparable to that of conventional chemical vapor deposition (CVD)-G/Si solar cells. This approach is done in air at low temperature, and is easy to scale up, making it appealing for the massive production of efficient and cost-effective G/Si solar cells.

Cite this: DOI: 10.1039/c0xx00000x

www.rsc.org/xxxxxx

ARTICLE TYPE

Efficient and Cost-effective Graphene on Silicon Solar Cells Prepared by Spray Coating

Kejia Jiao, DangWen Zhang, and Yunfa Chen*

Received (in XXX, XXX) Xth XXXXXXXXX 20XX, Accepted Xth XXXXXXXXX 20XX

DOI: 10.1039/b000000x

We demonstrate the first example of efficient and cost-effective graphene on silicon solar cells prepared using spray coating. The spray coating process is optimized by investigating the effects of substrate temperature and graphene film thickness on device performance. With the aid of a simple hydroquinone/methanol surface passivation method, spray-coated G/Si solar cells with power conversion efficiency of 4.41 % can be obtained. Our method is faster and simpler than conventional fabrication method, and is easy to scale up, highlighting their great potential in the massive production of efficient and low-cost G/Si solar cells.

Introduction

In the past decade, owing to the outstanding properties of graphene,[1] there is an enormously growing interesting in exploring its potential applications in energy-related fields, such as solar cells, phototransistors, and supercapacitors.[2-5] Recently, a new type of schottky junction solar cells, i.e., the graphene on silicon (G/Si) solar cells, has been heavily investigated.[2, 6-10] The power conversion efficiency (PCE) of G/Si solar cells have been pushed to > 14 % using chemical doping of graphene together with TiO_2 antireflection coating layer,[7] highlighting the great potential of G/Si solar cells. However, traditional fabrication process of G/Si solar cells necessitates high temperature chemical vapor deposition (CVD) growth of graphene and complicated transfer process,[11, 12] which make CVD-G/Si solar cells costly. In contrast, solution-processed graphene provides an alternative way to circumvent the aforementioned drawbacks. For example, Liu et al. report G/Si solar cells prepared by thermal reduction of graphene oxide (GO).[13] However, on one hand, the preparation of GO (i.e., the Hummer's method[14]) is dangerous and not environmentally friendly; on the other hand, the post-annealing step makes the fabrication process complicated, which inevitably increase the cost of G/Si solar cells. Graphene quantum dots (GQDs)/Si solar cells are also reported.[15] Again the synthesis and purification of GQDs is tedious and time-consuming. Therefore, there still lacks an effective method to fabricate efficient and cost-effective G/Si solar cells.

One important factor that leads to low PCE of pristine G/Si solar cells is the large interface recombination due to the presence of a large amount of surface dangling bonds on unpassivated silicon surface (here pristine refers to G/Si solar cells without any treatment, e.g., chemical doping of graphene and/or antireflection coating. In fact, the PCE of pristine G/Si soalr cells is typically around 2 % [6, 10]). Surface passivation can improve device performance since it can greatly reduce interface recombination. By now, two silicon surface passivation methods have been utilized in G/Si solar cells. The first one is the formation of a thin SiO_x layer.[6] The SiO_x layer tends to produce fixed sheet charge near the interface, giving rise to open-circuit voltage (V_{oc}).[16] However, the continued oxidation of SiO_x layer will do harm to the long-term stability of devices. The second one employs a two-step chlorination-alkylation method.[15, 17, 18] Though this method is widely used, the preparation process is hazardous and complicated. Therefore, a simple and environmental friendly silicon surface passivation method is highly desirable in G/Si solar cells.

Herein, we demonstrate a facile method to fabricate efficient and cost-effective G/Si solar cells. Spray coating is selected because it is suitable for industrial applications. The graphene solution is prepared by eletrochemical exfoliation, which has attracted attention due to its easy, fast and environmental friendly nature.[19-21] The effects of substrate temperature and graphene film thickness on device performance are investigated in details. Subsequently a very simple but effective hydroquinone/methanol approach is introduced to passivate the silicon surface, and spray-coated G/Si solar cell with PCE of 4.41 % can be obtained. These results thus serve as a model example towards efficient and cost-effective G/Si solar cells.

Experimental details

Electrochemical exfoliation of graphene. The exfoliation of graphene is done according to a previous report with little modification.[19] Briefly, graphite/copper foils are used as the anode/cathode, respectively. The inorganic salt solution used here is 0.1 M Na_2SO_4 solution. A 10 V positive voltage is applied to the graphite foil. After exfoliation, the as-synthesized product is collected by vacuum filtration, and washed copiously using deionized water and ethanol. After dried at 80 ^oC for several hours, the product is dissolved in DMF (~1.5 mg/ml) by sonication for 15 min. Finally, the graphene dispersion is

centrifuged at 1000 rpm for 60 min before use.

Silicon surface passivation. The silicon substrates are first cleaned using RCA process, followed by sonication in acetone, 2-propanol and deionized water, then a 1 min HF (2 %) dipping is applied. Finally they are treated with 0.01 M hydroquinone/methanol solution in dark for 3 h as reported elsewhere.[22]

Spray deposition of graphene. The graphene dispersion is sprayed onto preheated silicon substrates using an airbrush (KUSING BD, 0.2 mm) with head pressure of ~ 40 psi. The spray speed is 3 mL/min, and the distance between nozzle and substrates are ~ 15 cm, and the graphene film thickness is controlled by spray time.

Device Fabrication. N-type Si (2~4 Ω cm, with a square window of 0.1 cm^2 surrounded by 300 nm thick SiO_2) is used as substrates. After the spray deposition of graphene, Ag paste and Ga-In eutectic alloy are applied as the front and back electrodes, respectively.

Characterization Method. The graphene flakes are examined using scanning electronic microscope (SEM), Raman Spectrum, X-ray photoelectronic spectrascopy (XPS) and ultraviolet photoelectronic spectrascopy (UPS). SEM images are acquired with JSM-7001F. Raman Spectra are performed using Renishaw inVia microscope with 532 nm wavelength incident laser light. XPS and UPS data are taken with AXIS Ultra instrument from Kratos Analytical. UPS measurements are performed using an unfiltered HeI (21.22 eV) gas discharge lamp to determine the work function of samples. XPS measurements are made with a monochromatic Al K_α source (1486.6 eV). The graphene film thicknesses are measured by ellipsometer, SENTECH SE850, and the aperture diameter is 0.2 mm. The solar cells are tested uinder Air Mass 1.5G illumination (100 mW/cm^2, the light density is calibrated using a standard solar reference cell, SRC-1000-TC-QZ, VLSI Standards S/N: 10510-0305). The *J-V* data are recorded with a Keithley 2400 SourceMeter. IPCE is obtained using QTEST STATION 500AD in the range 300 nm ~1100 nm.

Results and Discussion

The fabrication of G/Si solar cells is accomplished in air at low temperature with the aid of spray coating (Fig. 1a). Besides, no post-annealing process is needed. These features make our method suitable for massive production. The graphite foil is first electrochemical exfoliated in an inorganic salt solution, [19 19] then the exfoliated graphene is dispersed in N,N′-dimethylformamide (DMF) to form graphene solution. The solution (Fig. 2, ~1.5 mg/mL) can stay stable for at least two weeks without apparent agglomeration. Fig. 1c depicts the Raman spectrum of graphene deposited on SiO_2/Si substrates. It shows an I_D/I_G ratio of 0.98, which is smaller than that for chemically/thermally reduced GO (1.1~1.5).[23] X-ray photoelectron spectroscopy (XPS) discloses a 15.18 atom % oxygen content, and careful examination of O 1S peak (Fig. S2) shows that 23.4% oxygen atoms come from DMF and Na_2SO_4. Therefore the C/O ratio of graphene is estimated to be 82.59/(15.18×(1-0.23)) = 7.06. Deconvoluted C 1S peak (Fig. 1d) reveals the presence of 4.63 atom % of C-OH (285.4 eV), 5.35 atom % of C-O (286.6 eV) and 1.65 atom % atom of C=O (287.9 eV) groups. The morphology of graphene is observed by SEM (Fig. S3), it is shown that most graphene flake sizes are in the range of several micrometers.

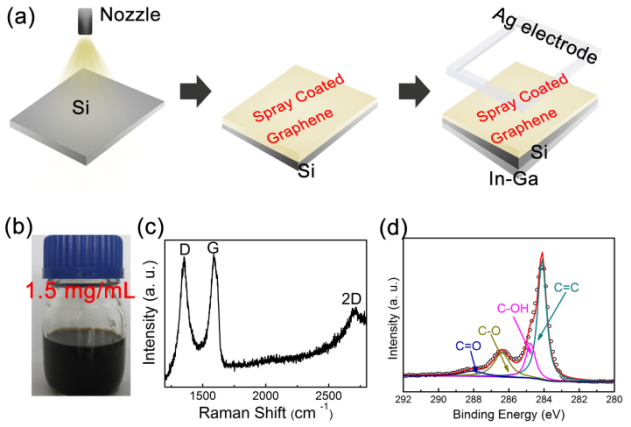

Fig. 1. (a) Schematic illustration of the fabrication process of spray-coated G/Si solar cells. (b) Dispersed graphene in DMF solution (concentration: ~ 1.5 mg/mL). (c) Raman Spectrum of electrochemical exfoliated graphene. (d) Deconvoluted C 1S peak showing the oxygen-containing group.

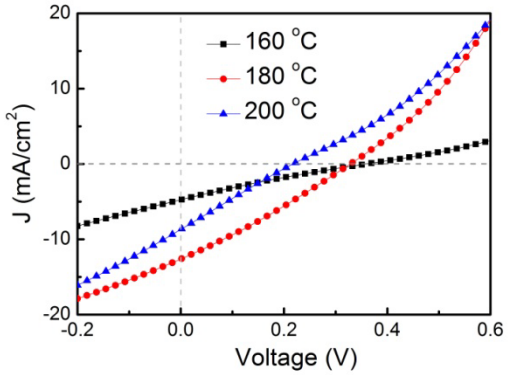

Fig. 2. The effects of T_{sub} on device performance.

Table 1. Photovoltaic parameters of solar cells in Fig. 1.

Sub.Temp. (°C)	J_{sc} (mA/cm^2)	V_{oc} (V)	FF	PCE (%)
160 (black curve)	4.5	0.35	0.24	0.47
180 (red curve)	12.6	0.31	0.3	1.16
200 (blue curve)	7.3	0.2	0.25	0.37

The graphene solution is first spray-coated onto preheated pristine (untreated) silicon substrates. Since substrate temperature (T_{sub}) is a critical factor in spray deposition,[24] the effects of T_{sub} on device performance are studied. As shown in Fig. 2 and Table 1, the PCE is more than doubled when T_{sub} is increased from 160 °C to 180 °C, mainly due to the increase in J_{sc} (from 4.5 to 12.6 mA/cm^2) even though V_{oc} is slightly decreased (a decrease of 11.4 %). Further increasing T_{sub} (200 °C) will cause degradation in device performance as a result of decrease in J_{sc} and V_{oc} from 12.6 to 7.3 mA/cm^2 and 0.31 to 0.2 V, respectively. In order to have reliable results, each set of devices are fabricated with three parallel cells and the statistical results of J_{sc},V_{oc} and PCE are plotted in Fig. 3a (see Table S1 for details, there are little changes in FF (see Fig. S4) and therefore not shown here). As seen, there exists a clear trend of decreasing V_{oc} with increasing T_{sub} (red curve). In schottky junction solar cells, V_{oc} is related to the schottky barrier height (SBH). According to Schottky-Mott model, the SBH at the G/Si interface is related to the difference between

the graphene work function WF_G and the electron affinity χ_{Si} of silicon by the equation, SBH = $WF_G - \chi_{Si}$.[25] Ultraviolet Photoelectron Spectroscopy (UPS, Fig. 3b) show that WF_G gradually decreases with increasing T_{sub}. WF_G is respectively 4.87, 4.82 and 4.72 eV at 160, 180 and 200 °C. The differences in WF_G match well with the variations in V_{oc}, which implies that the changes in V_{oc} are due to the changes in WF_G. The changes in WF_G are explained by taking the graphene film chemical compositions into account. XPS are performed to probe the chemical compositions of graphene and the results are listed in Fig. 3c. It is obvious that the C/O ratio increases (oxygen content decreases) as T_{sub} increases. Higher oxygen content in graphene leads to higher WF_G due to the fact that the larger electronegativity of oxygen atoms produces surface $C^{\delta+}$-$O^{\delta-}$ dipoles *via* extraction of electrons from graphene.[26] The variations in J_{sc} can be explained as follows. Under the same illumination conditions (AM 1.5G) and using graphene with the same thickness (by controlling spray time), J_{sc} can be expressed as $J_{sc} = f(\beta, SBH)$, where β is the quantum efficiency.[27] β can be estimated from incident photon-to-electron conversion efficiency (IPCE) spectra. As shown in Fig. 3d, $IPCE_{180} > IPCE_{200} > IPCE_{160}$, which means that the largest β is obtained at 180 °C. As discussed above, SBH decreases with increasing T_{sub}. As a consequence, the highest J_{sc} is obtained at 180 °C. In the following study, T_{sub} is fixed at 180 °C.

The effects of graphene film thickness (δ) on device response are also investigated and there clearly exists an optimal thickness for device performance. δ is measured at three different points and fitted using Tauc-Lorentz Model. The mean square errors (MSE) in all cases are smaller than 1, indicating the applicability of this model in our case. Fig. 4a gives the variations of PCE with δ (see Table S2 and S3 for detailed device parameters). As seen, δ mainly affects J_{sc}. When the graphene film is very thin (2.46 nm), J_{sc} is very low (~0.05 mA/cm^2); J_{sc} is enhanced by about two order of magnitudes (~ 6 mA/cm^2) when δ is increased to 15.89 nm. The highest J_{sc} is obtained at 26.30 nm (12.3 mA/cm^2), and further increase in δ (36.78 nm) causes decrease in J_{sc} (7.4 mA/cm^2). The variation trend of J_{sc} with δ is the same as that of IPCE (Fig. 6b), indicating that recombination at the interface is the main factor determining J_{sc}. It further confirms the conclusion that in our case, J_{sc} is the most critical parameter that dominates PCE.

Since the recombination at the interface limits J_{sc} and hence the overall PCE, surface passivation can improve the PCE significantly in this situation. Here a hydroquinone/methanol surface passivation method is employed. Compared to the widely used chlorination-alkylation method, the routine used here is much simpler and more environmental friendly. XPS and UPS spectra are performed to confirm the successful surface modification. As shown in the C 1s spectra (Fig. S8), a new peak located at ~286.7 eV appeared after surface modification, which is attributed to C-O bonding.[28] The doublet $Si2p_{3/2}$ and $Si2p_{1/2}$ at 99.3 and 99.9 eV show clear attenuation (Fig. 5a), indicating the formation of a monolayer on silicon.[29] The treated sample shows lower amplitude of oxidized Si (102~104 eV, the red rectangle) than pristine Si, indicating that it is more stable and more resistant to oxidation in ambient. The WF of pristine and treated samples is respectively 4.07 and 3.72 eV as obtained from UPS

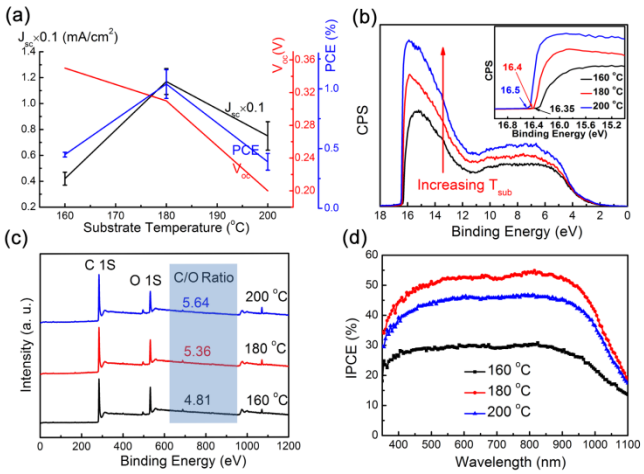

Fig. 3. (a) Statistical results of device photovoltaic parameters: J_{sc} and V_{oc}. (b) UPS spectra of graphene deposited at different T_{sub}. The inset is an amplification of curve edge in the range of 17~16 eV. Obviously the WF of graphene decreases with increasing T_{sub}. (c) XPS spectra of graphene deposited at different T_{sub}. The C/O ratio is indicated in the blue shadow. It increases as T_{sub} increases. (d) The IPCE curve of solar cells fabricated at different T_{sub}. The highest IPCE is obtained at 180 °C.

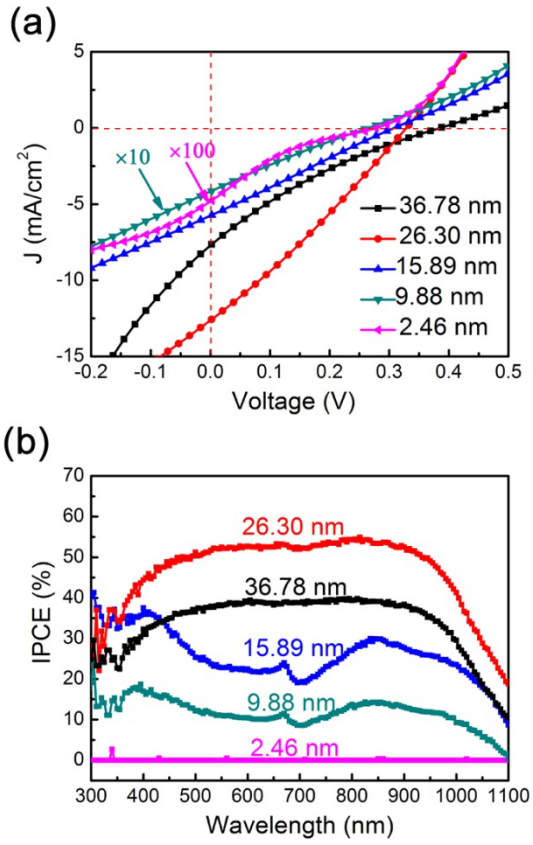

Fig. 4. (a) The change of PCE with δ. (b) The corresponding IPCE curves.

spectra (Fig. 5b). It means that the electron affinity (χ) of treated sample is lowered by 350 meV (the inset of Fig. 5b) compared to that of pristine sample. As shown later, the decreased χ enhances the schottky barrier height (SBH), leading to higher V_{oc} and FF. The XPS and UPS together demonstrate the successful surface modification.

The PCE of spray-coated G/Si solar cell can reach 4.41 % using

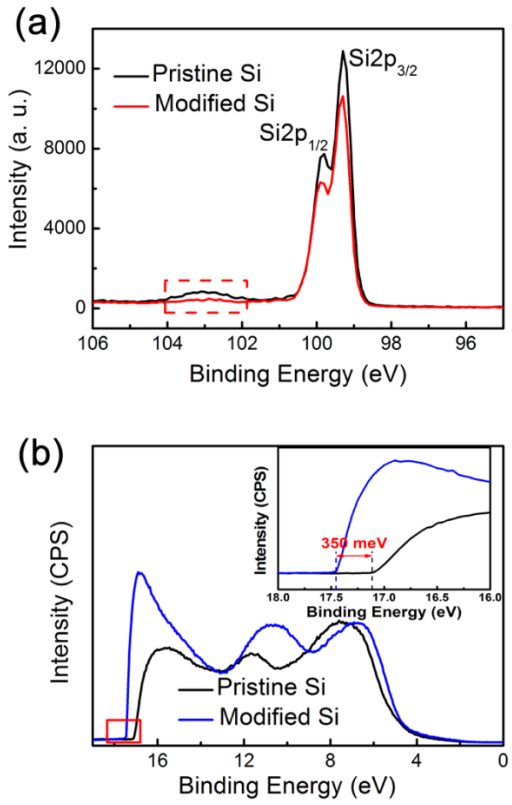

Fig. 5. (a) Si 2p spectra of pristine/modified silicon. The doublet $Si2p_{3/2}$ and $Si2p_{1/2}$ at 99.3 and 99.9 eV show clear attenuation, indicating the formation of a monolayer on silicon. (b) UPS spectra of pristine/modified silicon. The inset shows that the electron affinity (χ) of modified silicon is lowered by 350 meV compared to pristine silicon.

hydroquinone-treated silicon as the substrate (Fig. 6a, red curve). An increase of ~ 300 % in PCE is obtained after surface passivation, as a result of the increase in J_{sc}, V_{oc} and FF from 12.6 to 23.8 mA/cm^2, 0.3 to 0.46 V, and 0.3 to 0.46 respectively. The IPCE curves of pristine/modified Si/G solar cells are given in Fig. 6b. It is clear that after surface modification, the recombination at Si/G interface is reduced (i.e., higher IPCE is indicative of lower interface recombination[30]). Besides, the SBH is increased after surface passivation, which leads to more efficient charge separation and higher V_{oc}.[25] The reduced recombination at Si/G interface and the more efficient charge separation both contribute to the better FF. Figure 7 gives the dark I-V curves of pristine/modified devices, and the insets show the calculations of series resistance (R_s, the upper) and shunt resistance (R_{sh}, the lower). R_s is extracted from the dV/d(lnI) VS I plot from the forward dark I-V curves using the Cheung method[31] and R_{sh} is calculated from the dark reverse bias I-V curves. As seen, R_s decreases from 285.2 to 81.9 Ω, while R_{sh} increases from 116.4 to 213.6 Ω after surface modification. The decrease in R_s and the increase in R_{sh} both lead to a higher PCE. It should be pointed out that the PCE of spray-coated G/Si is comparable to that of CVD-G/Si solar cells, yet this method is much simpler and faster.

Conclusions

In summary, we demonstrate efficient and cost-effective G/Si solar cells fabricated by spray coating. The effects of substrate temperature and graphene film thickness on device response are investigated in details. The PCE of G/Si can reach 4.41 % using hydroquinone-treated silicon as substrates. It is believed that the PCE can be further improved using higher quality graphene (i.e., larger flakes and fewer defects) and further treatments (e.g., chemical doping). This method is much simpler and faster than the conventional fabrication method, and is easy to scale up, which potentially open up new opportunities for the massive production of efficient and low-cost G/Si solar cells.

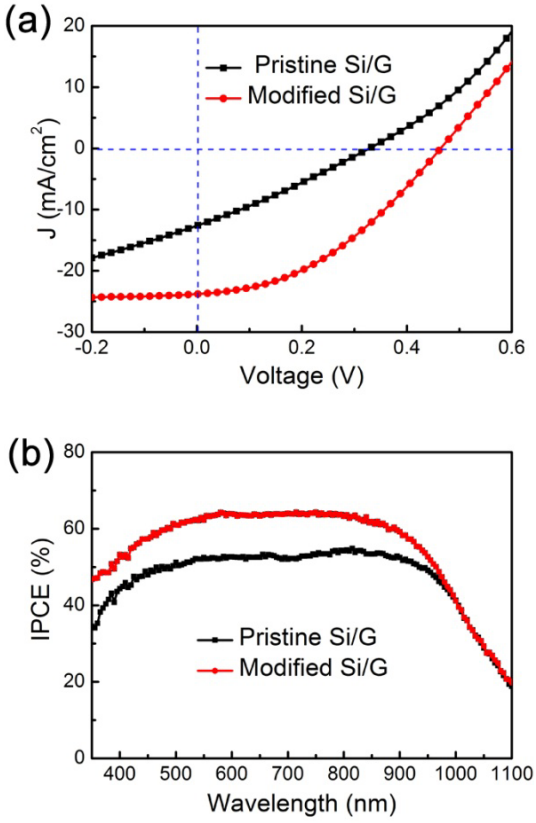

Fig. 6. (a) *J-V* curves of pristine/modified Si/G solar cells. The PCE of G/Si solar cells is increased from 1.12% to 4.41% after surface modification. (b) The corresponding IPCE curves.

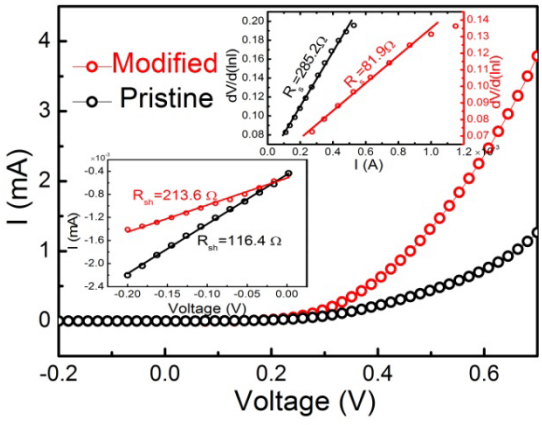

Fig. 7. The dark I-V curves of pristine/modified Si/G solar cells. The insets show the calculations of series resistance (R_s, the upper) and shunt resistance (R_{sh}, the lower). R_s decreases from 285.2 to 81.9 Ω, while R_{sh} increases from 116.4 to 213.6 Ω after surface modification.

Acknowledgement

The authors gratefully acknowledge the supports from Strategic Leading Science & Technology Programme (Grant No. XDB0505000), and the 863 Hi-tech Research and Development Program of China (2010AA064903).

Notes and references

K. J. Jiao, D.W. Zhang, and Prof. Y. F. Chen

State Key Laboratory of Multiphase Complex Systems, Institute of Process Engineering, Chinese Academy of Sciences Beijing 100190 (P.R. China)

E-mail: chenyf@home.ipe.ac.cn

†Electronic Supplementary Information (ESI) available: [Fig. S1~S8, Table S1 to S3]. See DOI: 10.1039/b000000x/

1. A. K. Geim, *Science*, 2009, **324**, 1530.
2. X. M. Li, H. W. Zhu, K. L. Wang, A. Y. Cao, J. Q. Wei, C. Y. Li, Y. Jia, Z. Li, X. Li and D. H. Wu, *Adv. Mater.*, 2010, **22**, 2743.
3. G. Konstantatos, M. Badioli, L. Gaudreau, J. Osmond, M. Bernechea, F. P. G. de Arquer, F. Gatti and F. H. L. Koppens, *Nat. Nanotechnol.*, 2012, **7**, 363.
4. H. Wang, Y. Yang, Y. Liang, J. T. Robinson, Y. Li, A. Jackson, Y. Cui and H. Dai, *Nano Lett.*, 2011, **11**, 2644.
5. K. S. Novoselov, V. I. Fal'ko, L. Colombo, P. R. Gellert, M. G. Schwab and K. Kim, *Nature*, 2012, **490**, 192.
6. X. C. Miao, S. Tongay, M. K. Petterson, K. Berke, A. G. Rinzler, B. R. Appleton and A. F. Hebard, *Nano Lett.*, 2012, **12**, 2745.
7. E. Shi, H. Li, L. Yang, L. Zhang, Z. Li, P. Li, Y. Shang, S. Wu, X. Li, J. Wei, K. Wang, H. Zhu, D. Wu, Y. Fang and A. Cao, *Nano Lett.*, 2013, **13**, 1776.
8. X. H. An, F. Z. Liu and S. Kar, *Carbon*, 2013, **57**, 329.
9. G. F. Fan, H. W. Zhu, K. L. Wang, J. Q. Wei, X. M. Li, Q. K. Shu, N. Guo and D. H. Wu, *Acs. Appl. Mater. Inter.*, 2011, **3**, 721.
10. T. X. Cui, R. T. Lv, Z. H. Huang, S. X. Chen, Z. X. Zhang, X. Gan, Y. Jia, X. M. Li, K. L. Wang, D. H. Wu and F. Y. Kang, *J. Mater. Chem. A*, 2013, **1**, 5736.
11. X. S. Li, W. W. Cai, J. H. An, S. Kim, J. Nah, D. X. Yang, R. Piner, A. Velamakanni, I. Jung, E. Tutuc, S. K. Banerjee, L. Colombo and R. S. Ruoff, *Science*, 2009, **324**, 1312.
12. K. S. Kim, Y. Zhao, H. Jang, S. Y. Lee, J. M. Kim, K. S. Kim, J.-H. Ahn, P. Kim, J.-Y. Choi and B. H. Hong, *Nature*, 2009, **457**, 706.
13. Q. M. Liu, F. Wanatabe, A. Hoshino, R. Ishikawa, T. Gotou, K. Ueno and H. Shirai, *Jpn. J. Appl. Phys.*, 2012, **51**.
14. M. Hirata, T. Gotou, S. Horiuchi, M. Fujiwara and M. Ohba, *Carbon*, 2004, **42**, 2929.
15. P. Gao, K. Ding, Y. Wang, K. Ruan, S. Diao, Q. Zhang, B. Sun and J. Jie, *J. Phys. Chem. C*, 2014, **118**, 5164.
16. D. R. Lillington and W. G. Townsend, *Appl. Phys. Lett.*, 1976, **28**, 97.
17. C. Xie, X. Z. Zhang, Y. M. Wu, X. J. Zhang, X. W. Zhang, Y. Wang, W. J. Zhang, P. Gao, Y. Y. Han and J. S. Jie, *J. Mater. Chem. A*, 2013, **1**, 8567.
18. Y. Wu, X. Zhang, J. Jie, C. Xie, X. Zhang, B. Sun, Y. Wang and P. Gao, *J. Phys. Chem. C*, 2013, **117**, 11968.
19. K. Parvez, Z. S. Wu, R. J. Li, X. J. Liu, R. Graf, X. L. Feng and K. Mullen, *J. Am. Chem. Soc.*, 2014, **136**, 6083.
20. J. H. Lee, D. W. Shin, V. G. Makotchenko, A. S. Nazarov, V. E. Fedorov, Y. H. Kim, J.-Y. Choi, J. M. Kim and J.-B. Yoo, *Adv. Mater.*, 2009, **21**, 4383.
21. C.-Y. Su, A.-Y. Lu, Y. Xu, F.-R. Chen, A. N. Khlobystov and L.-J. Li, *ACS Nano*, 2011, **5**, 2332.
22. H. Takato, I. Sakata and R. Shimokawa, *Jpn. J. Appl. Phys.*, 2002, **41**, L870.
23. L. Buglione, E. L. K. Chng, A. Ambrosi, Z. Sofer and M. Pumera, *Electrochem. Commun.*, 2012, **14**, 5.
24. F. C. Krebs, *Sol. Energy Mater. Sol. Cells*, 2009, **93**, 394.
25. M. Sze and K. K. Ng, *Physics of Semiconductor Devices (3rd edition)*, Wiley, Hoboken, 2007.
26. C.-W. Chen and M.-H. Lee, *Diamond Relat. Mater.*, 2003, **12**, 565.
27. N. Swami, S. Srivastava and H. Ghule, *J. Phys. D: Appl. Phys.*, 1979, **12**, 765.
28. R. Har-Lavan, O. Yaffe, P. Joshi, R. Kazaz, H. Cohen and D. Cahen, *AIP Adv.*, 2012, **2**.
29. S. P. Pujari, E. van Andel, O. Yaffe, D. Cahen, T. Weidner, C. J. van Rijn and H. Zuilhof, *Langmuir*, 2013, **29**, 570.
30. X. Li, D. Xie, H. Park, T. H. Zeng, K. Wang, J. Wei, M. Zhong, D. Wu, J. Kong and H. Zhu, *Adv. Energy Mater.*, 2013, **3**, 1029.
31. S. K. Cheung and N. W. Cheung, *Appl. Phys. Lett.*, 1986, **49**, 85.